Speed sensorless adaptive rotor flux orientation control of induction motor drive

Ji juan[1], Yanliang Cui[1], and Kaiyun Wang[2]

[1]Lanzhou Jiaotong University
[2]Southwest Jiaotong University

October 9, 2023

Abstract

This article investigates a sensorless indirect rotor flux orientation control (IRFOC) for induction motors based on stator resistance and slip angular speed deviation. An estimation method of rotor flux and speed based only on stator three-phase current and voltage measurements is proposed. An adaptive approximation method of voltage model and current model with stator voltage compensation method is considered to estimate the rotor flux and to accurately locate the flux angle in the case of stator resistance deviation. In addition, the stator current deviation due to the slip angle speed deviation is taken into account in the speed estimation, and the rotor speed indirect estimator (RSIE) is designed, which can adjust the slip angle speed in real time according to the changes of current and flux to reduce the dependence on the accurate model and parameters. Alternatively, Simulink simulation is utilized to verify the practicality and reliability of the proposed induction motor rotor flux and speed estimator method.

Hosted file

`figure1.eps` available at https://authorea.com/users/672721/articles/671674-speed-sensorless-adaptive-rotor-flux-orientation-control-of-induction-motor-drive

Hosted file

`figure2.eps` available at https://authorea.com/users/672721/articles/671674-speed-sensorless-adaptive-rotor-flux-orientation-control-of-induction-motor-drive

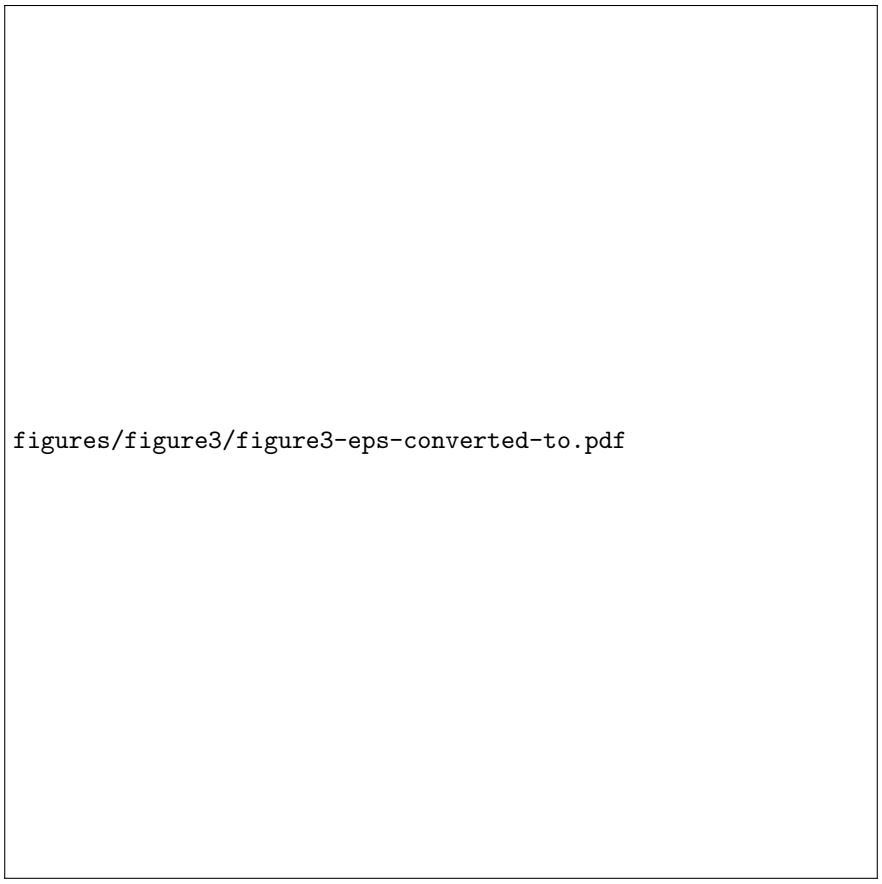

Hosted file

figure4.eps available at https://authorea.com/users/672721/articles/671674-speed-sensorless-adaptive-rotor-flux-orientation-control-of-induction-motor-drive

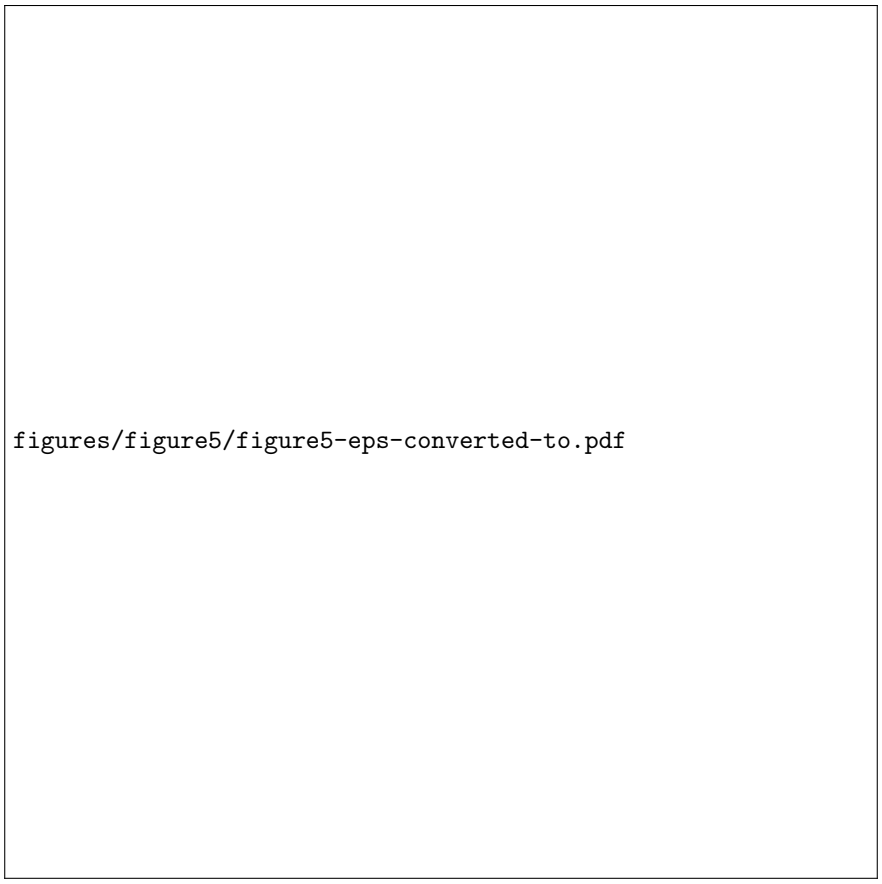

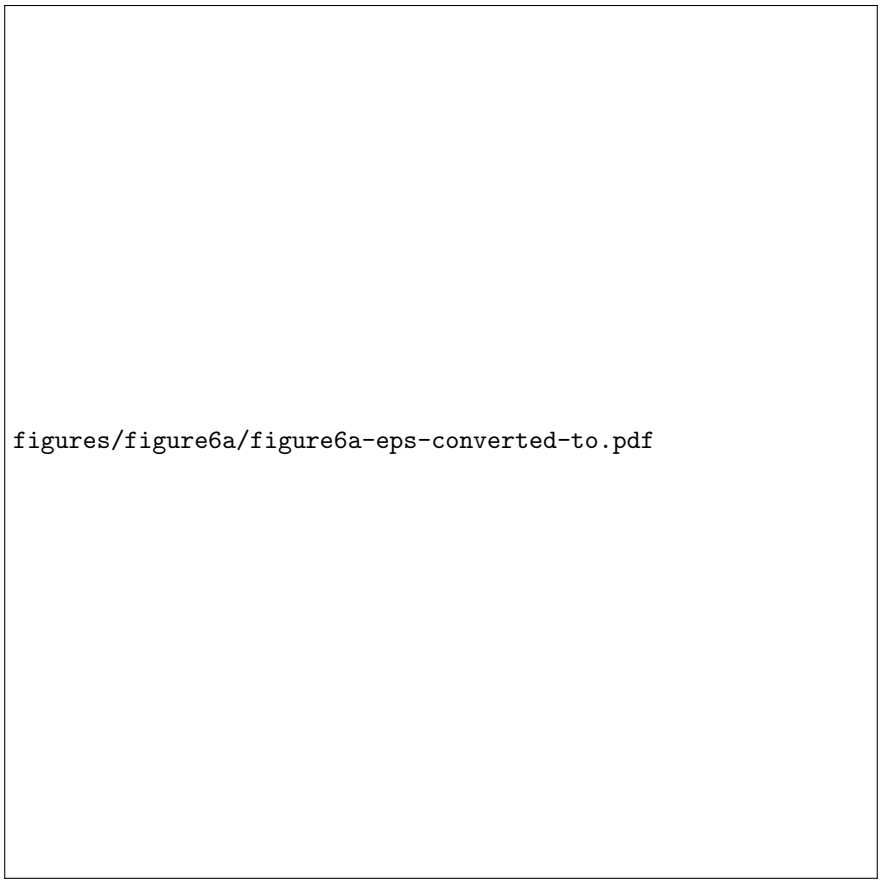

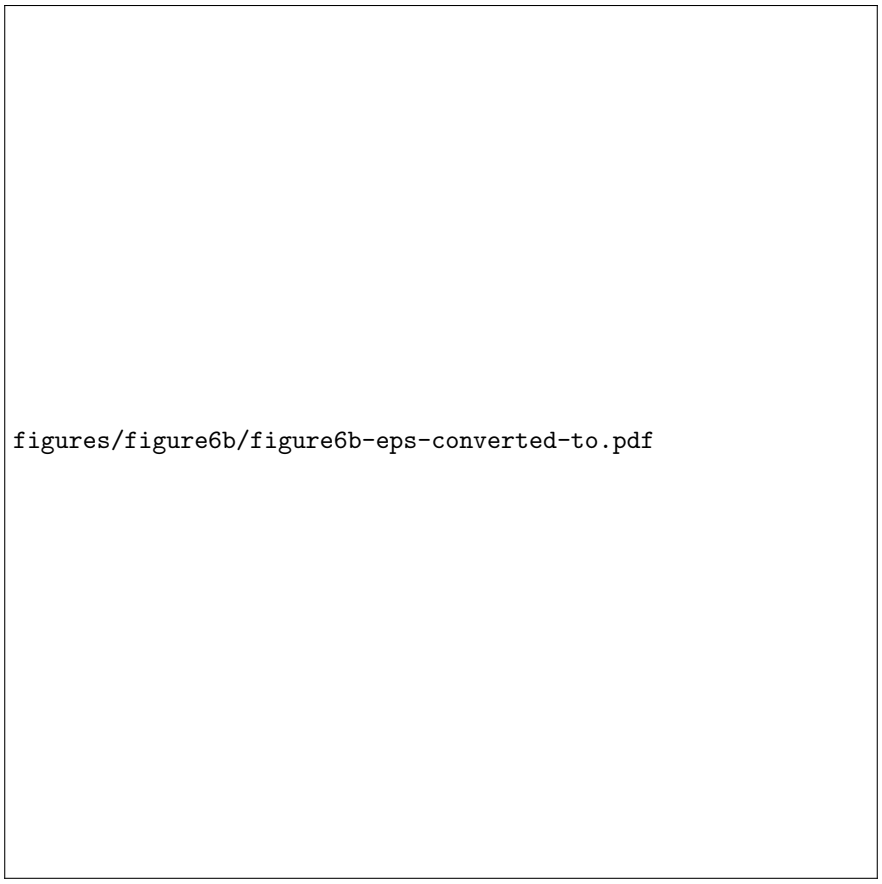

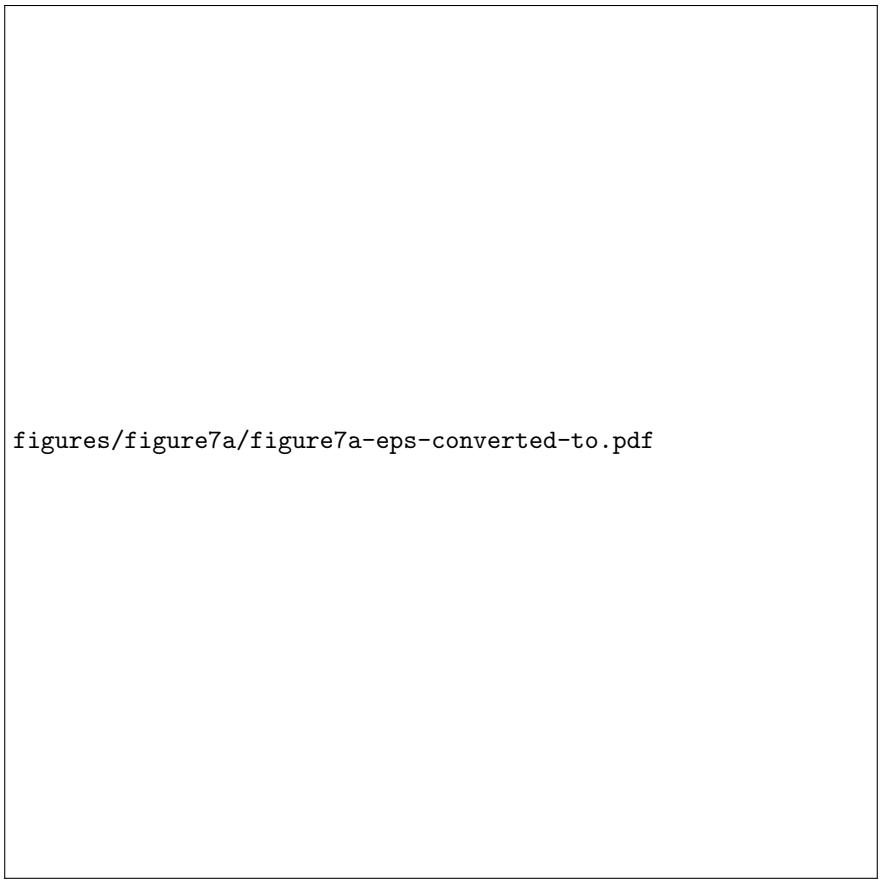

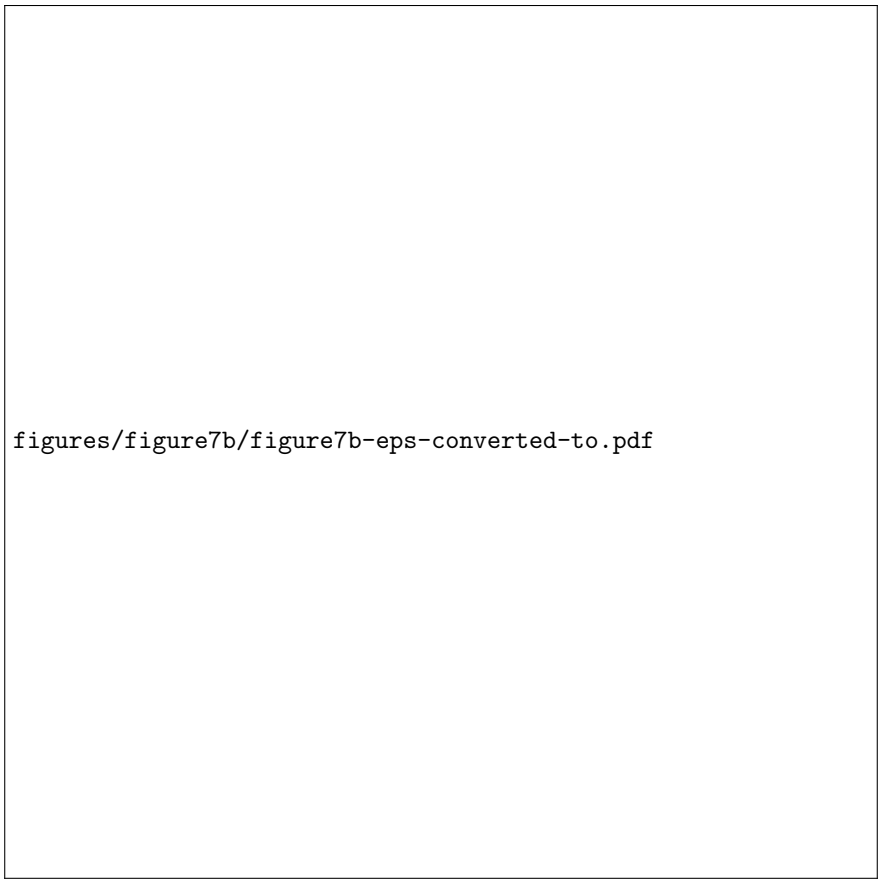

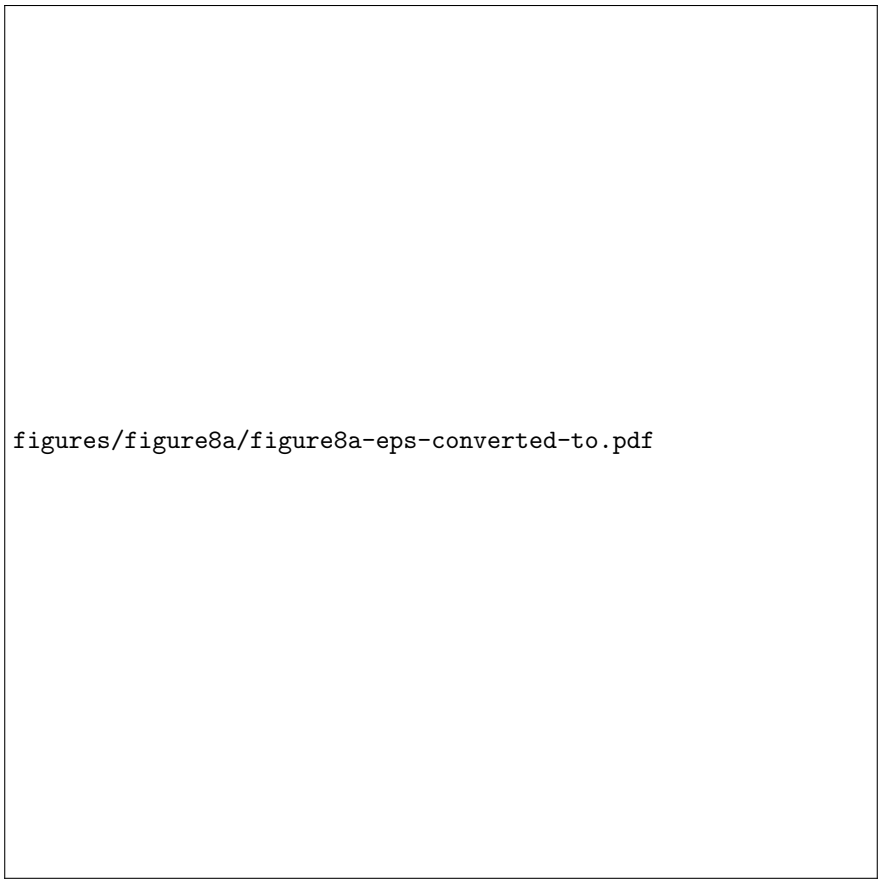

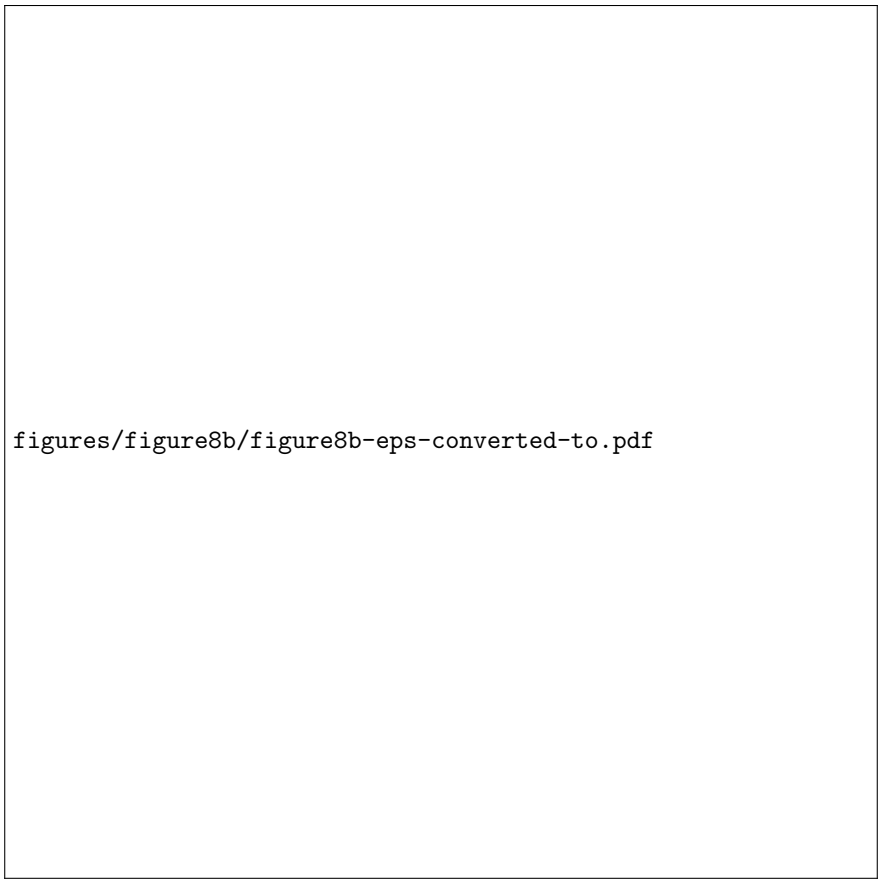

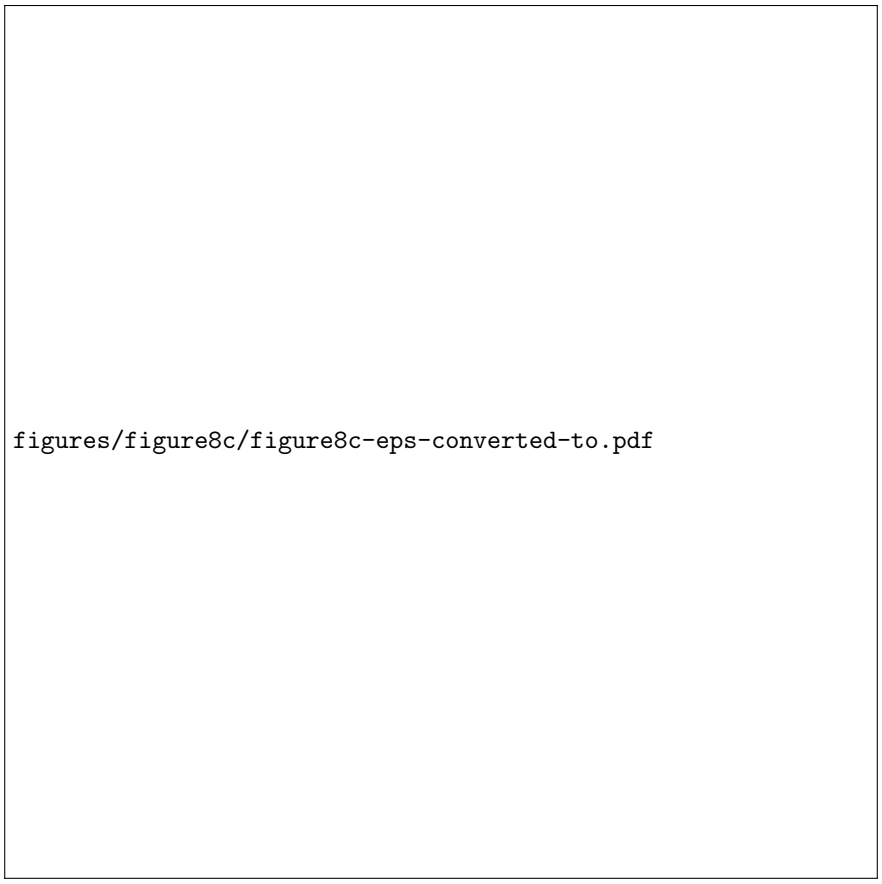

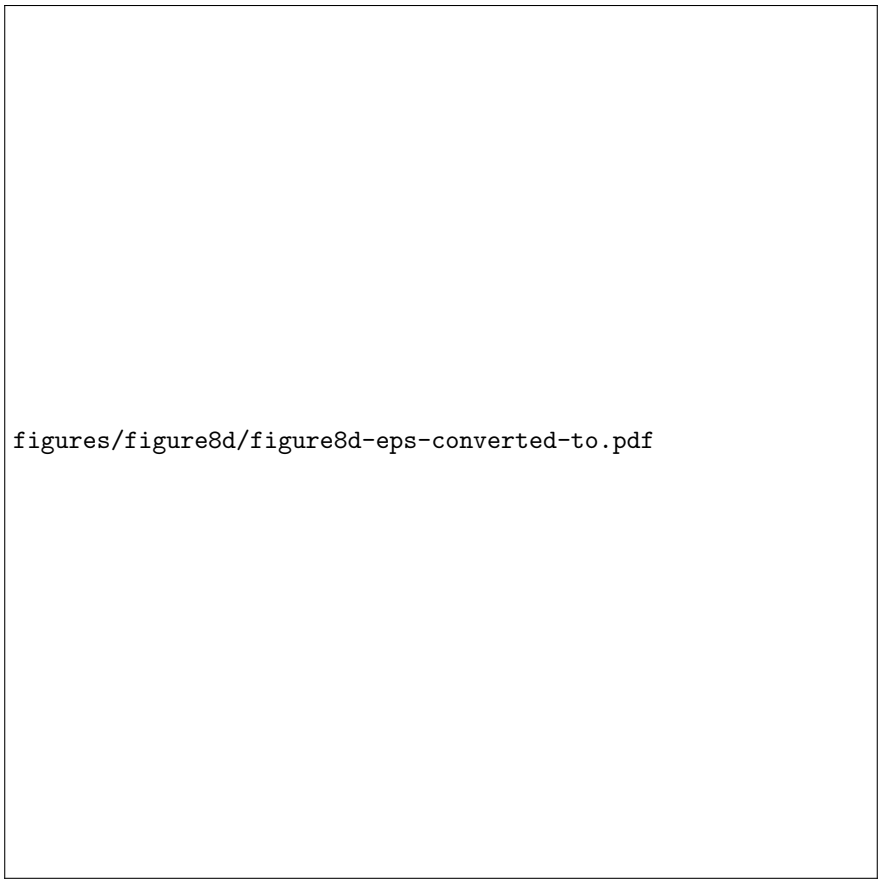

Hosted file

figure9.eps available at https://authorea.com/users/672721/articles/671674-speed-sensorless-adaptive-rotor-flux-orientation-control-of-induction-motor-drive

Speed sensorless adaptive rotor flux orientation control of induction motor drive

Juanjuan Ji[a], Yanliang Cui[a,*], Kaiyun Wang[b,*]

[a]*School of Mechanical Engineering, Lanzhou Jiaotong University, Lanzhou 730070, Gansu, China*
[b]*State Key Laboratory of Rail Transit Vehicle System, Southwest Jiaotong University, Chengdu 610031, Sichuan, China*

Abstract

This article investigates a sensorless indirect rotor flux orientation control (IRFOC) for induction motors based on stator resistance and slip angular speed deviation. An estimation method of rotor flux and speed based only on stator three-phase current and voltage measurements is proposed. An adaptive approximation method of voltage model and current model with stator voltage compensation method is considered to estimate the rotor flux and to accurately locate the flux angle in the case of stator resistance deviation. In addition, the stator current deviation due to the slip angle speed deviation is taken into account in the speed estimation, and the rotor speed indirect estimator (RSIE) is designed, which can adjust the slip angle speed in real time according to the changes of current and flux to reduce the dependence on the accurate model and parameters. Alternatively, Simulink simulation is utilized to verify the practicality and reliability of the proposed induction motor rotor flux and speed estimator method.

Keywords: sensorless control, induction motor, stator resistance deviation, flux and speed estimators.

1. Introduction

The flux orientation control (FOC), also known as vector control, is universally employed in speed regulation or torque control for induction motors [1]-[8]. As with DC motors, speed control of induction motors is an operational requirement placed on motors by production machinery to improve productivity and product quality, conserve energy, and improve service quality. FOC controls the speed or torque of an induction motor by controlling the stator current space vector. It accurately controls the magnitude and direction of the flux, resulting in a motor with smooth torque, low noise, high efficiency, and high-speed dynamic response. Due to the obvious advantages of FOC, it has been gradually replacing the traditional control methods in many applications, and has attracted much attention in the motion control industry [9]-[15]. FOC techniques can be divided into two categories: direct and

*Corresponding author, Email: 1124530496@qq.com

indirect flux orientation control schemes. For the direct FOC method, the stator end is used to obtain the flux vector, while the indirect control method uses the motor slip frequency to realize the flux orientation. However, the performance of FOC for induction motors directly affects the performance of current control. Therefore, how to accurately locate the flux angle of an induction motor is crucial for controlling the rotor speed.

Induction motor traction drive systems require high performance controllers for fast transient response and smooth operation. A typical motor control system is to transform a nonlinear system into a linear system, which can realize the complete decoupling of rotor speed and flux [16]-[18]. This method can regulate both speed and flux simultaneously without neglecting the nonlinear dynamics of speed and flux coupling. Based on this method, a series of methods for speed control of induction motors have been proposed, such as the model linearization process [19],[20], which can fully linearize the flux and the rotational speed in order to decouple their dynamics. and nonlinear model predictive control to solve the optimal control problem [21]-[26]. The main drawback of linearized control methods is the need for a detailed system model and precise model parameters. In practice, the complex and variable system operating environment makes it difficult to accurately obtain the motor parameters, such as the time-varying rotor and stator resistances [18],[27],[28]. This greatly reduces the robustness and reliability of linear control methods. To address this problem, researchers have developed disturbance estimation and compensation methods based on nonlinear adaptive control [29]. These methods perform online estimation and compensation of a centralized disturbance term containing nonlinear parts, external disturbances and parameter variations. Therefore, its performance does not depend on the accuracy of the IM model. In addition, there are online parameter estimation techniques [30]-[32] that compensate for stator voltage variations by estimating the resistive voltage drop from the stator temperature. In recent work, it can be found that the problem of accurately obtaining the parameters of the motor has aroused intense discussions among many scholars.

On the other hand, all high-performance vector-controlled induction motor drives require precise speed or rotor position information for feedback control. This information is provided by incremental encoders, and the use of such sensors means more electronics, higher costs, and much lower overall system reliability. In some cases, it is difficult to install, such as for motor drives in harsh environments and at high speeds, which undoubtedly increases weight, size and electrical sensitivity. In order to overcome these problems, a lot of research has been done in recent years on speed estimation for sensorless control. For example, in the literatures [29] and [33], a nonlinear adaptive controller without speed sensors is proposed to simultaneously estimate the speed, rotor flux phase by utilizing a third-order extended state observer. In literature [34], an integral sliding mode control method based on a nonlinear model of the rotor counter electromotive force is used to achieve sensorless FOC flux angle positioning of the motor under rotating conditions. A predictive current delay compensation control algorithm is proposed in literature [35], which introduces the concept of virtual voltage vector to provide more accurate flux as well as phase angle for the motor without increasing the computational complexity of the processor. In summary, it can be seen that the core of FOC is the indirect calculation or estimation of the rotor flux and the precise positioning of the rotor flux angle. Among them, the precise positioning of the flux

angle is the key factor. In order to realize the accurate positioning of the flux angle, common methods include phase-locked loop and PI tracking control. For example, in the literatures [36]-[38], a third-order PLL with a steady-state linear Kalman filter is utilized to track the flux angle without deviation to achieve dynamic adjustment to harmonic disturbances and parameter changes. In order to solve the problem of accurate positioning of the flux angle, it is necessary to propose a sensorless speed FOC control strategy to ensure accurate positioning of the flux angle as well as bias-free following of the rotor speed.

In the aforementioned literature, the authors mostly focus on decoupling the rotor flux and speed as well as speed estimation design methods to reduce nonlinearities and coupling and improve system reliability. However, the most existing flux and speed estimators are usually designed as complementary and compatible conditions for open-loop system stability. It means that the flux estimator and speed estimator are designed independently. More significantly, the complexity of the motor operating environment leads to parameter deviation. That is, if the parameter variations are not taken into account in time, accurate positioning of the flux angle and precise control of the speed are meaningless because the motor parameters cannot be accurately acquired. However, up to now, the above problems have not been adequately addressed yet.

Motivated by the above literature reviews, this article further investigates an indirect rotor flux orientation control induction motor system with a hybrid adaptive approximate estimator for rotor flux and a rotor speed indirect estimator. The main contributions of this work are summarized as follows:

- 1) Different with the most existing literatures, an adaptive approximation method is mainly proposed by only utilizing voltage and current measurements to evaluate the rotor flux. At the same time, the stator resistance parameter deviation is also considered, and the stator voltage compensation method is used to compensate for the resistance voltage drop caused by the resistance deviation.

- 2) A speed sensorless indirect estimator is designed to estimate the rotor speed by indirectly calculating the flux angle and estimating the slip angular speed. Using the rotor speed estimated by RSIE to compensate for the deviation value of slip angular speed, in order to reduce the dependence on accurate models and parameters, and improve the robustness of FOC control methods.

Nomenclature

u_{sd}, u_{sq}	d, q-axis stator voltage components.	L_m	Mutual inductance.
i_{sd}, i_{sq}	d, q-axis stator current components.	n_p	Number of pole pairs.
$\varphi_{sd}, \varphi_{sq}$	d, q-axis stator flux components.	J	Moment of inertia.
$\varphi_{rd}, \varphi_{rq}$	d, q-axis rotor flux components.	f_v	Friction constant.
ω_s, ω_r	Synchronous and rotor angular speed.	τ_r	Rotor time constant.
R_s, R_r	Stator and rotor resistance.	ω_{sl}	Slip angular speed.
L_s, L_r	Stator and rotor self-inductance.	T_e	Electromagnetic torque.

K_P	Proportional gain of stator voltage compensator.	T_L	Load torque.
		$\wedge$	Estimated value.
K_I	Integral gain of stator voltage compensator.	$*$	Reference value.
		Δ	Deviation value.

The remainder of the paper is organized as follows. Section 2 gives a detailed dynamic model of the induction motor in the d-q frame. The sensorless speed control scheme is described in Section 3. Section 4 gives a simulation example. Conclusion remarks are outlined in Section 5.

2. Rotor flux orientation control model

The dynamic model of an asynchronous motor can be represented by the common d-axis and q-axis components in a synchronous rotating frame. Usually, the cage motor is considered, and its internal rotor is in a short-circuit state. A typical flux dynamic of asynchronous motor can be described as the following [29]-[38]:

$$\begin{cases} \dfrac{d\varphi_{sd}}{dt} = -R_s i_{sd} + \omega_s \varphi_{sq} + u_{sd} \\ \dfrac{d\varphi_{sq}}{dt} = -R_s i_{sq} - \omega_s \varphi_{sd} + u_{sq} \\ \dfrac{d\varphi_{rd}}{dt} = -R_r i_{rd} + \omega_{sl} \varphi_{rq} \\ \dfrac{d\varphi_{rd}}{dt} = -R_r i_{rd} + \omega_{sl} \varphi_{rq} \end{cases} \tag{1}$$

Fig. 1 shows the block diagram of the proposed sensorless IRFOC flux and speed estimators of the induction motor drive system. The control system consists of rotor speed estimator, improved rotor flux estimator, a RFOC control block, a V/F SVPWM pulse width modulator and inverter.

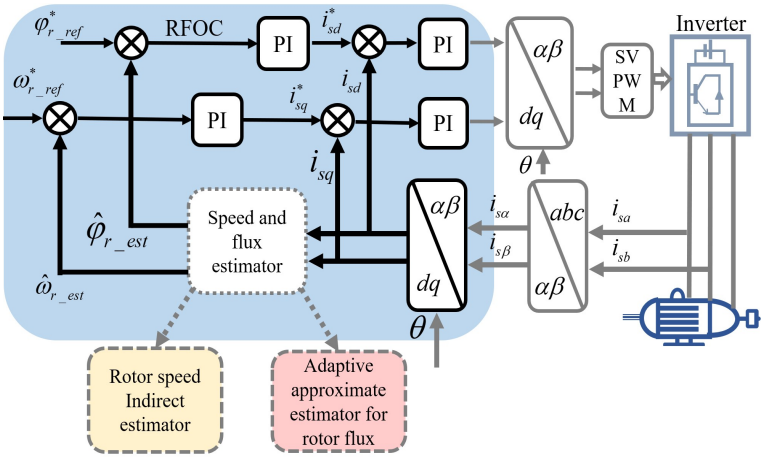

Fig. 1: The control framework of the RFOC for IM

The goal of the indirect rotor field-oriented control (RFOC) of an asynchronous motor is to make the flux and torque control similar to that of the separately excitation DC motor, where these parameters are controlled independently. In this way, the directional rotor flux contains the following conditions:

$$\begin{cases} \varphi_{rd} = \varphi_d \\ \varphi_{rq} = 0 \end{cases} \tag{2}$$

Besides, the torque (power invariant transformation) of an induction motor is given as [3]-[6]:

$$T_e = \frac{n_p L_m}{L_r}(i_{sq}\varphi_{rd} - i_{sd}\varphi_{rq}) \tag{3}$$

According to Eq. (1), Eq. (2) and Eq. (3), flux and torque furthermore can be written as:

$$\begin{cases} \varphi_{rd} = \dfrac{L_m}{\tau_r s + 1} i_{sd} \\ T_e = \dfrac{n_p L_m}{L_r} \varphi_{rd} i_{sq} \end{cases} \tag{4}$$

Usually, the motion equations are given as the following equation:

$$T_e - T_L - f_v \omega_r = J\frac{d\omega_r}{dt} \tag{5}$$

$$\omega_s = \omega_r + \omega_{sl} \tag{6}$$

Then slip angular speed equation is written as:

$$\omega_{sl} = \frac{L_m}{\tau_r \varphi_{rd}} i_{sq} \tag{7}$$

3. Sensorless speed control algorithm

3.1. Adaptive approximate estimator for rotor flux

As shown in Fig. 2, in the proposed scheme, an adaptive approximate estimator (AAE) is employed to obtain an estimate of the rotor flux. AAE can be viewed as the flux estimator that consists of the voltage model and the current model acting together in combination. It can be clearly seen that the calculation of the stator flux is crucial for accurately obtaining the rotor flux. In practice, the performance of the voltage model for flux estimation in the low-speed region is not ideal due to the presence of the pure integrator and stator resistance deviation. On the contrary, in the medium and high-speed region, the flux values estimated by the current model are not satisfactory due to the deviation of the rotor parameter. Considering this situation, AAE makes full use of the advantages of both models and avoids their disadvantages to estimate the rotor flux better. Besides, AAE has the advantages of simple implementation, robustness and acceptable performance.

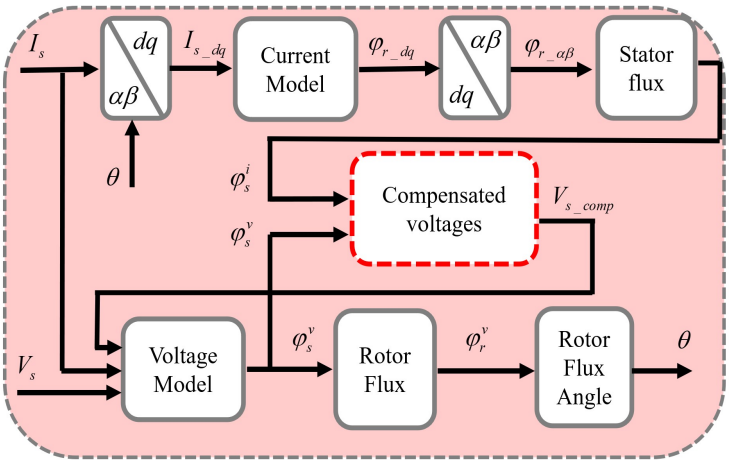

Fig. 2: Adaptive approximate estimator for rotor flux

The voltage model of the induction motor in the $\alpha\beta$-frame is written as follows:

$$\begin{cases} \begin{bmatrix} \varphi_{r\alpha}^v \\ \varphi_{r\beta}^v \end{bmatrix} = -\dfrac{L_s L_r - L_m^2}{L_m} \begin{bmatrix} i_{s\alpha} \\ i_{s\beta} \end{bmatrix} + \dfrac{L_r}{L_m} \begin{bmatrix} \varphi_{s\alpha}^v \\ \varphi_{s\beta}^v \end{bmatrix} \\ \begin{bmatrix} \varphi_{s\alpha}^v \\ \varphi_{s\beta}^v \end{bmatrix} = \begin{bmatrix} \int (u_{s\alpha} - R_s i_{s\alpha}) dt \\ \int (u_{s\beta} - R_s i_{s\beta}) dt \end{bmatrix} \end{cases} \tag{8}$$

where $\varphi_{r\alpha}^v$ is the α-axis component of the rotor flux in the voltage model, $\varphi_{r\beta}^v$ is the β-axis component of the rotor flux in the voltage model, and $\varphi_{s\alpha}^v$ is the α-axis component of the stator flux in the voltage model, $\varphi_{s\alpha}^v$ is the β-axis component of the stator flux in the voltage model.

From Eq. (8), the stator flux vector $\varphi_{s\alpha\beta}^v$ is estimated as the integral of the voltage drop in the stator resistance subtracted from the stator voltage vector. It is evident that due to the presence of pure integrators and stator resistance, the performance of the voltage model may be affected by DC voltage deviate and changes in stator resistance. Therefore, it is necessary to discuss the impact of stator resistance deviation on the accurate acquisition of rotor flux.

In order to correctly select the variables that can identify the stator resistance variations, a graphical study of the d-axis and q-axis current errors as a function of stator resistance has been carried out. As can be seen in Fig. 3, the d-axis current error varies approximately linearly with the stator resistance ΔR_s. The q-axis current error remains weak and negligible compared to the d-axis current error. Therefore, only the d-axis current error is used to estimate the variation of stator resistance.

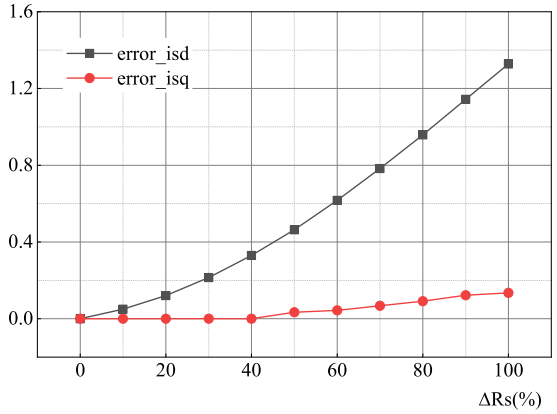

Fig. 3: d-axis and q-axis current error with stator resistance variation

Subsequently, the stator flux equation after stator resistance deviation becomes as follows:

$$\begin{bmatrix} \tilde{\varphi}^v_{s\alpha}(t) \\ \tilde{\varphi}^v_{s\beta}(t) \end{bmatrix} = \begin{bmatrix} \int (u_{s\alpha} - R_s i_{s\alpha} + \Delta R_s i_{s\alpha}) dt \\ \int (u_{s\beta} - R_s i_{s\beta} + \Delta R_s i_{s\beta}) dt \end{bmatrix} \tag{9}$$

The stator flux is shifted during the voltage model calculation due to the stator resistance at low speeds and long-term operation. In addition to this, purely integral terms due to DC voltage offset and phase errors degrade the accuracy of rotor flux calculations. In order to avoid such errors, various methods are available to improve the voltage-based flux observer, commonly low-pass filters, high-pass filters, etc. In this paper, a stator voltage compensator is designed to greatly improve the bias due to stator resistive voltage drop and pure integrator. In order to ensure the estimation performance of the rotor flux, a compensation unit is introduced in the voltage model, represented as:

$$\begin{bmatrix} \hat{\varphi}^v_{s\alpha}(t) \\ \hat{\varphi}^v_{s\beta}(t) \end{bmatrix} = \begin{bmatrix} \int (u_{s\alpha} - R_s i_{s\alpha} + \Delta R_s i_{s\alpha} - u_{com,s\alpha}) dt \\ \int (u_{s\beta} - R_s i_{s\beta} + \Delta R_s i_{s\beta} - u_{com,s\beta}) dt \end{bmatrix} \tag{10}$$

Accordingly, the stator voltage compensator is designed as follows:

$$\begin{aligned} u_{com,s\alpha} &= K_P(\varphi^v_{s\alpha} - \varphi^i_{s\alpha}) + K_I \int (\varphi^v_{s\alpha} - \varphi^i_{s\alpha}) dt \\ u_{com,s\beta} &= K_P(\varphi^v_{s\beta} - \varphi^i_{s\beta}) + K_I \int (\varphi^v_{s\beta} - \varphi^i_{s\beta}) dt \end{aligned} \tag{11}$$

where $\varphi^i_{s\alpha}$ is the α-axis component of the stator flux in the current model, and $\varphi^i_{s\beta}$ is the β-axis component of the stator flux in the current model.

Then, the stator flux obtained from the current model can be further calculated as follows:

$$\begin{bmatrix} \varphi^i_{s\alpha} \\ \varphi^i_{s\beta} \end{bmatrix} = \frac{L_s L_r - L_m^2}{L_r} \begin{bmatrix} i_{s\alpha} \\ i_{s\beta} \end{bmatrix} + \frac{L_r}{L_m} \begin{bmatrix} \varphi^i_{r\alpha} \\ \varphi^i_{r\beta} \end{bmatrix} \tag{12}$$

According to the Eq. (12), it is necessary to obtain the rotor flux under the current model, which is φ_r^i. Thus, the rotor flux provided by the Eq. (4) in the dq-frame can be obtained as:

$$\begin{bmatrix} \varphi_{rd}^i \\ \varphi_{rq}^i \end{bmatrix} = \begin{bmatrix} \dfrac{L_m}{\tau_r s + 1} i_{sd} \\ 0 \end{bmatrix} \tag{13}$$

where φ_{rd}^i is the d-axis component of the rotor flux in the current model, and φ_{rq}^i is the q-axis component of the rotor flux in the current model. Due to $i_{rq} = 0$, according to the formula $\varphi_{rq}^i = L_r i_{rq} + L_m i_{sq}$, it can be inferred that $\varphi_{rq}^i = 0$.

Alternatively, based on the inverse Park transformation, the rotor flux in the $\alpha\beta$ coordinate system can be obtained as:

$$\begin{bmatrix} \varphi_{r\alpha}^i \\ \varphi_{r\beta}^i \end{bmatrix} = \begin{bmatrix} \varphi_{rd}^i \cos\theta - \varphi_{rq}^i \sin\theta \\ \varphi_{rd}^i \sin\theta + \varphi_{rq}^i \cos\theta \end{bmatrix} \tag{14}$$

where φ_{rd}^i is the α-axis component of the rotor flux in the current model, and φ_{rq}^i is the β-axis component of the rotor flux in the current model.

Therefore, the rotor flux estimated using AAE can be obtained as:

$$\begin{bmatrix} \hat{\varphi}_{r\alpha}^v \\ \hat{\varphi}_{r\beta}^v \end{bmatrix} = -\frac{L_s L_r - L_m^2}{L_m} \begin{bmatrix} i_{s\alpha} \\ i_{s\beta} \end{bmatrix} + \frac{L_r}{L_m} \begin{bmatrix} \hat{\varphi}_{s\alpha}^v \\ \hat{\varphi}_{s\beta}^v \end{bmatrix} \tag{15}$$

From the above equations (8)-(15), it can be found that the basic idea of the adaptive approximate estimator for rotor flux is to dominate the voltage model stator flux. The difference between the voltage model and the current model is controlled by the PI, which in turn compensates for the voltage model. It is worth noting that IRFE mainly estimates the stator flux here, and the rotor flux is calculated from the stator flux and stator current, without directly estimating the rotor flux.

3.2. Rotor speed indirect estimator

In the vector control system of induction motor, the closed-loop control of speed is necessary, which is the guarantee of control stability and control performance. But the additional speed sensor will not only increase the cost of the system, but also affect the speed measurement accuracy if the sensor is installed improperly [39]-[42]. Moreover, the installation of the sensor will increase the axial volume of the motor, it brings some difficulties to the daily maintenance of the motor, and the speed sensor will reduce the mechanical robustness of the motor, and the precision of the sensor will be affected in the high temperature and high humidity environment. Based on these shortcomings, in order to overcome the above problems, this paper studies the speed sensorless vector control method. The structural diagram of the rotor speed estimator is shown in Figure 4.

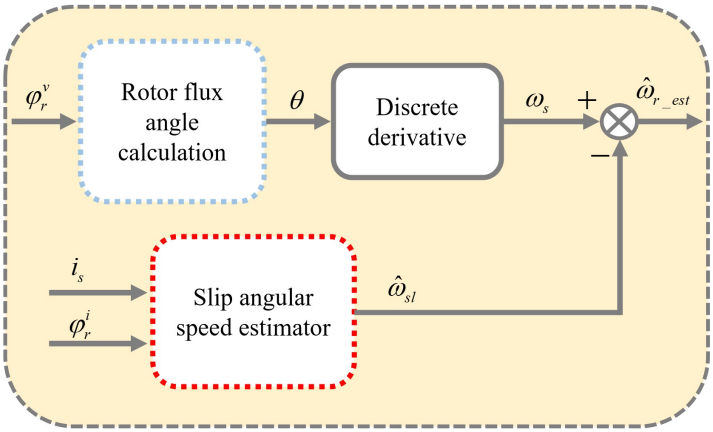

Fig. 4: Rotor speed indirect estimator

3.2.1. Rotor flux angle calculation

The slip angular speed ω_{sl} is added to the estimated rotor speed $\hat{\omega}_r$ to generate rotor synchronous angular speed ω_s,which means $\omega_s = \omega_{sl} + \hat{\omega}_r$.

Subsequently, if the discrete derivative calculation is performed on the rotor flux angle θ, the rotor synchronous angular speed ω_s can be given by

$$\omega_s = \frac{d\theta}{dt} \tag{16}$$

The position θ is used in the d-q transformation and the V/F PWM inverter blocks to calculate the d-q axis current and the SVPWM pattern, respectively. Therefore, it is evident that the rotor flux angle θ and slip angular speed ω_{sl} have to be estimated to obtain the rotor speed.

For clarity, the rotor flux angle is calculated from the voltage model component of the rotor flux, and the vector of the rotor flux angle is given as follows:

$$\theta = tan^{-1}\left(\frac{\hat{\varphi}_{r\beta}^v}{\hat{\varphi}_{r\alpha}^v}\right) \tag{17}$$

Thus, substituting the estimated value of Eq. 15 into Eq. 17 allows for the calculation of the space vector value of the rotor flux angle θ. Finally, substituting the calculated value of Eq. 17 into Eq. 16 can obtain the rotor synchronous angular speed.

3.2.2. Slip angular speed estimation

Due to the effects of unexpected road variation, such as uneven road surfaces, roadbed drops, road gradients, etc., the slip angular speed is actually changed along with the road. From Eq. 7, it can be found that under the condition that the rotor flux is kept balanced and unchanged, the slip angular speed varies linearly with the change of stator q-axis current. In order to verify the above linear change, the change rule of stator current error with the error of slip angular speed is investigated by graphical method [18], as shown in Fig. 5. From the figure, it can be seen that the change of q-axis current error with the slip angular

speed error is almost linear, while the d-axis current error is weak and negligible relative to the q-axis change.

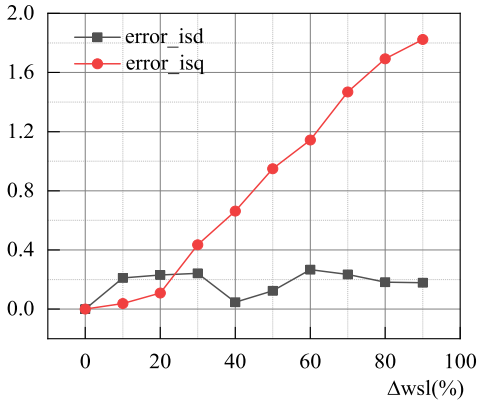

Fig. 5: d-axis and q-axis current error with slip angular speed variation

Alternatively, it can be seen that the stator q-axis current has to be obtained in order to obtain the slip angular speed from Eq. 7. There are two ways to obtain the q-axis current: the torque T_e or the slip angular speed ω_{sl}. In fact, $T_e = \varphi_{rd}^2 \omega_{sl}$, the electromagnetic torque T_e and the slip angular speed ω_{sl} are actually the same thing. It is clear that how to obtain the electromagnetic torque T_e and the rotor flux φ_r is the core content of RFOC. There are many methods in other literature [18],[33]-[35] that can estimate the slip angular speed ω_{sl}.

As a consequence, it is necessary to design a dynamic speed estimator because the stator q-axis current will deviate with the deviation of the slip angular speed. The calculation of the slip angular speed can be adjusted according to the change of stator current, which can effectively reduce the stator current error caused by the slip speed deviation. The dynamic speed estimator is derived based on the dynamic Park equation of the motor, and the expression for the slip angular speed is obtained from the mathematical equations of the electromagnetic relationship and rotor speed definition of the motor. The derivation method is based on the closed-loop estimation of the flux and the open-loop calculation of the speed.

Accordingly, the rotor flux is estimated from the current model, and the slip angular speed can be estimated by the following equation:

$$\omega_{sl} \approx \frac{1}{(\varphi_{r,\alpha\beta}^i)^2} \frac{L_m}{\tau_r} (\varphi_{r\alpha}^i i_{s\beta} - \varphi_{r\beta}^i i_{s\alpha}) \tag{18}$$

where $\varphi_{r,\alpha\beta}^i = \sqrt{(\varphi_{r\alpha}^i)^2 + (\varphi_{r\beta}^i)^2}$.

In light of the above, according to the equation $\omega_s = \omega_{sl} + \hat{\omega}_r$, the rotor speed $\hat{\omega}_r$ is estimated as follows:

$$\hat{\omega}_r = \omega_s - \omega_{sl} = \frac{d\theta}{dt} - \frac{1}{(\varphi_{r,\alpha\beta}^i)^2} \frac{L_m}{\tau_r} (\varphi_{r\alpha}^i i_{s\beta} - \varphi_{r\beta}^i i_{s\alpha}) \tag{19}$$

Remark 1: In the rotor speed based indirect estimator RSIE, the rotor speed can be obtained from the algebraic operation of the motor equations of motion. In the equations of motion, the synchronous speed is obtained from the differential calculation of the flux angle, while the flux angle localization is precisely obtained from the rotor flux voltage model calculation. In addition, the acquisition of the slip angular speed is the key step. Due to the deviation of the slip angular speed, the stator q-axis current is caused to be deviated consequently. Thus, in order to compensate for the deviation value of the slip angular speed, PI tracking control is used in the calculation to adjust the size of the slip angular speed in time with the current change. As a result, the dynamic calculation of the slip angular speed promptly eliminates the problem of parameter deviation. In the whole estimator design process, the algebraic calculation of the data information in two different loops greatly increases the tolerance and robustness of the speed estimator.

3.3. Performance analysis of control schemes

3.3.1. Stability under stator resistance deviation

The voltage equation and current equation of the stator flux can be obtained from formulas (8) and (12), respectively. It is obvious that the voltage equation is suitable for high-frequency use, and the current equation is suitable for low-frequency use. To achieve adaptive control of the flux based on frequency, this article proposes a hybrid adaptive approximation method, as shown in Figure 2. In this way, the closed-loop transfer function is obtained as follows:

$$\varphi_s = \frac{s^2}{s^2 + K_P s + K_I}\varphi^v_{s,\alpha\beta} + \frac{K_P s + K_I}{s^2 + K_P s + K_I}\varphi^i_{s,\alpha\beta} \tag{20}$$

It is known that Laplace's plural variable $s = j\omega$, the stator voltage $u_{s\alpha}, u_{s\beta}$ and current $i_{s\alpha}, i_{s\beta}$ used to generate the stator flux are rotated at the synchronous angular speed of the power supply $\omega_s = 2\pi f_s$. Since the voltage and current of the stator are changing from low to high frequency, that is, low frequency starting and high frequency speed regulation, the obtained stator flux $\varphi^i_{s\alpha}$ and $\varphi^i_{s\beta}$ are all quantities that vary with frequency. It can be seen that in the above PI control scheme, 1) low-frequency current-type flux, $\varphi^i_{s,\alpha\beta}$ in action, 2) high-frequency voltage flux, $\varphi^v_{s,\alpha\beta}$ in action.

From the above equation (9), when there is a deviation in the stator resistance, the deviation of the stator flux is $\Delta\varphi_{s,R_s} = \dfrac{s}{s^2 + K_P s + K_I}\Delta R_s i_{s\alpha\beta}(s)$.

Given that $i_{s\alpha}(s)$ and $i_{s\beta}(s)$ are always orthogonal, there must be:

$$\begin{cases} i_{s\alpha}(t) = i_s sin(\omega_s t) \\ i_{s\beta}(t) = i_s cos(\omega_s t) \end{cases} \longrightarrow \begin{cases} i_{s\alpha}(s) = i_s \dfrac{\omega_s^2}{s^2 + \omega_s^2} \\ i_{s\beta}(s) = i_s \dfrac{s^2}{s^2 + \omega_s^2} \end{cases} \tag{21}$$

Thus, it is possible to obtain:

$$\begin{cases} \Delta\varphi_{s\alpha} = \dfrac{s}{s^2 + K_P s + K_I} \Delta R_s i_s \dfrac{s}{s^2 + \omega_s^2} \\ \Delta\varphi_{s\beta} = \dfrac{s}{s^2 + K_P s + K_I} \Delta R_s i_s \dfrac{\omega_s}{s^2 + \omega_s^2} \end{cases} \tag{22}$$

From here, the error of steady state is as follows

$$\begin{cases} \Delta\varphi_{s\alpha,ess} = \lim\limits_{s\to 0} s\Delta\varphi_{s\alpha} = 0 \\ \Delta\varphi_{s\beta,ess} = \lim\limits_{s\to 0} s\Delta\varphi_{s\beta} = 0 \end{cases} \tag{23}$$

Therefore, it is obvious that the desired control effect of vector control can be well achieved by using stator flux PI control with the stator resistance deviation.

3.3.2. Stability under slip angular speed deviation

From Fig. 5 and Eq. (7), it is not difficult to observe that when the slip angular speed is deviated, the stator q-axis current is also deviated. The deviation of the stator current will inevitably lead to the deviation of the stator flux. Adopting the same PI adaptive control method, the transfer function remains as Eq. (20). When the slip angular speed deviates, the stator flux equation becomes:

$$\begin{bmatrix} \bar{\varphi}_{s\alpha}^{v} \\ \bar{\varphi}_{s\beta}^{v} \end{bmatrix} = \begin{bmatrix} \int (u_{s\alpha} - R_s i_{s\alpha} + u_{\Delta\omega_{sl}}) dt \\ \int (u_{s\beta} - R_s i_{s\beta} + u_{\Delta\omega_{sl}}) dt \end{bmatrix} \tag{24}$$

The transfer function becomes the following equation:

$$\varphi_{s,\omega_{sl}} = \frac{s^2}{s^2 + K_P s + K_I} (\varphi_{s,\alpha\beta}^{v} + \frac{1}{s} u_{\Delta\omega_{sl}}) + \frac{K_P s + K_I}{s^2 + K_P s + K_I} \varphi_{s,\alpha\beta}^{i} \tag{25}$$

Thus, the deviation of the flux becomes:

$$\Delta\varphi_s = \varphi_s - \varphi_{s,\omega_{sl}} = \frac{s^2}{s^2 + K_P s + K_I} \frac{1}{s} u_{\Delta\omega_{sl}} = \frac{s}{s^2 + K_P s + K_I} u_{\Delta\omega_{sl}} \tag{26}$$

Accordingly, the steady state error can be obtained as:

$$\Delta\varphi_{s,ess} = \lim_{s\to 0} s\Delta\varphi_s = \lim_{s\to 0} \frac{s^2}{s^2 + K_P s + K_I} u_{\Delta\omega_{sl}}(s) = \lim_{s\to 0} \frac{u_{\Delta\omega_{sl}}(s)}{K_I} \tag{27}$$

Therefore, it can be known that when the slip angular speed deviates, it directly leads to the deviation of the stator flux, and the RFOC effect is bound to deteriorate. Change method: add another first-order integral to make the deviation amount $\Delta\tilde{\varphi}_s = \dfrac{s}{s^2 + K_P s + K_I} \dfrac{1}{s} u_{\Delta\omega_{sl}}$, resulting in a steady state error of zero. In other words, it is necessary to add another integral control after the stator voltage PI control to eliminate the slip angular speed deviation.

3.3.3. Stability under PI control

When the states i_{sd} and i_{sq} of the motor system can be obtained directly, as well as the state ω_r of the mechanical system can be estimated, the objectives to be controlled are: 1) the estimated rotor speed $\hat{\omega}_r$ arrives at its reference value ω_r^*; 2) the estimated rotor flux $\hat{\varphi}_{rd}$ arrives at its reference value φ_{rd}^*. From Eq. (3), it can be seen that if the electromagnetic torque can be changed to Eq. (4) by controlling the rotor flux φ_{rq} to be 0. Assuming the given current reference values of i_{sd}^* and i_{sq}^*, equations (1-4) can be combined to obtain:

$$\frac{d}{dt}\begin{bmatrix}\hat{\omega}_r\\ \hat{\varphi}_{rd}\end{bmatrix} = \begin{bmatrix}\frac{n_p L_m}{J L_r}\hat{\varphi}_{rd} i_{sq}^* - \frac{f_v}{J} - \frac{T_L}{J}\\ \frac{R_r}{L_r}\hat{\varphi}_{rd} + \frac{R_r L_m}{L_r} i_{sd}^*\end{bmatrix} \tag{28}$$

The above system equation (24) gives a direct correlation $i_{sd}^* = \frac{L_r}{R_r L_m}\dot{\hat{\varphi}}_{rd} + \frac{1}{L_m}\hat{\varphi}_{rd}$ between the flux $\hat{\varphi}_{rd}$ and the current i_{sd}^*. Obviously, the current i_{sd}^* can be controlled by controlling the flux $\hat{\varphi}_{rd}$, but before that, a premise needs to be solved: controlling the flux φ_{rq} is 0. It is already known that $\varphi^* = \sqrt{\varphi_{rd}^2 + \varphi_{rq}^2}$, and it is evident that if $\hat{\varphi}_{rd}$ can be controlled to reach the φ_{rd}^*, that is, if the nominal flux φ^* is all projected onto the d-axis, $\varphi_{rq} = 0$ can naturally be guarantee. Comprehensively, it can be seen that the current i_{sd}^* can be reached with the following PI control:

$$i_{sd}^* = K_{P\varphi}(\varphi^* - \hat{\varphi}_{rd}) + K_{I\varphi}\int_0^t (\varphi^* - \hat{\varphi}_{rd}(s))ds + \frac{L_r}{R_r L_m}\dot{\varphi}^* + \frac{1}{L_m}\varphi^* \tag{29}$$

Among them, $K_{P\varphi}$ and $K_{I\varphi}$ represent the proportional and integral gains, respectively. The meaning of the control equation (25) is that the deviation $\varphi^* - \hat{\varphi}_{rd}$ tends towards 0 through PI control. When the deviation $\varphi^* - \hat{\varphi}_{rd}$ is not 0, the first half $K_{P\varphi}(\varphi^* - \hat{\varphi}_{rd}) + K_{I\varphi}\int_0^t (\varphi^* - \hat{\varphi}_{rd}(s))ds$ acts to drive the deviation value $\varphi^* - \hat{\varphi}_{rd}$ to be 0 eventually; and when the deviation reaches 0, the latter half $\frac{L_r}{R_r L_m}\dot{\varphi}^* + \frac{1}{L_m}\varphi^*$ acts to reach the estimated flux $\hat{\varphi}_{rd}$ and current i_{sd} are all nominal.

Defining the deviation $e_\varphi = \varphi^* - \hat{\varphi}_{rd}$, the control equation (25) is brought into equation (24) to obtain:

$$\dot{e}_\varphi = -\frac{R_r}{L_r}(1 + L_m K_{P\varphi})e_\varphi - \frac{R_r L_m}{L_r}K_{I\varphi}\int_0^t e_\varphi(s)ds \tag{30}$$

Define the vector $\chi_\varphi(t) = \begin{bmatrix}\int_0^t e_\varphi(s)ds\\ e_\varphi(t)\end{bmatrix}$ to obtain the equation of state:

$$\dot{\chi}_\varphi(t) = A_\varphi \chi_\varphi(t) \tag{31}$$

where $A_\varphi = \begin{bmatrix}0 & 1\\ -\frac{R_r L_m}{L_r}K_{I\varphi} & -\frac{R_r}{L_r}(1 + L_m K_{P\varphi})\end{bmatrix}$.

It can be seen that changing the parameters $K_{P\varphi}$ and $K_{I\varphi}$ can make A_φ a Hurwitz matrix, and the system (27) must be stabilized, which can realize the flux adaptive control.

4. Simulation results

In MATLAB/Simulink environment, the performance of the induction motor based on the speed sensorless vector controller is verified by using the motor parameters shown in Appendix Table 1. The performance of an induction motor based on a sensorless indirect rotor flux orientation control (IRFOC) is verified in the MATLAB/Simulink environment, and the system simulation model is shown in Fig. 6. The motor parameters used in the simulation process are shown in Table 1.

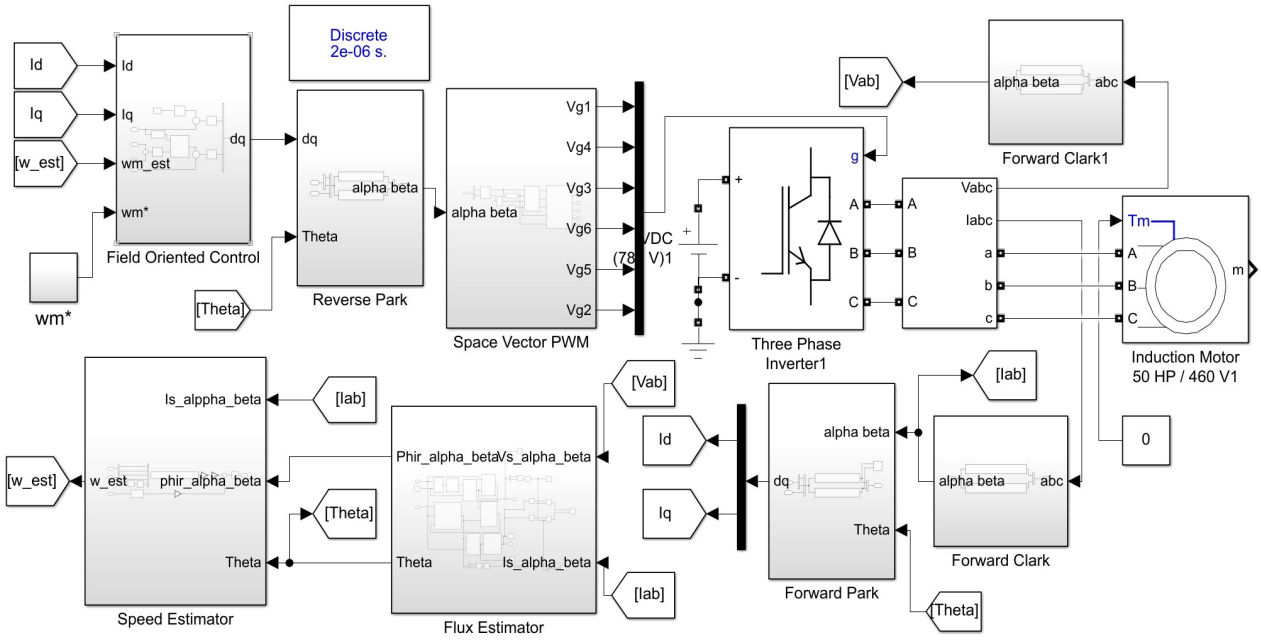

Fig. 6: System simulation model

Table 1: Motor parameters

Specification		Parameters	
Rated power	$37.3kw$	R_s	0.287Ω
Rated voltage	$460V$	R_r	0.228Ω
Rated frequency	$50Hz$	L_s	$0.0348H$
Number of pole pairs	2	L_r	$0.0355H$
Rated speed	$1500r/min$	L_m	$0.0347H$
Sampling time	$2e-6$	J	$0.662kg.m^2$
		f	$0.1Nm.s.rad^{-1}$

In order to validate the improved rotor flux estimator based on stator resistance deviation and the rotor speed estimator based on slip angular speed deviation proposed in this article, a RFOC for a sensorless IM drive is constructed using MATLAB/Simulink and the validity and feasibility of the methodology is verified. Extensive simulation results are provided, especially in using the novel estimator to control very low rotor speed with multiple

consecutive accelerations and decelerations to simulate the simulation of a real control system. The RFOC scheme uses the estimated speed signals as the speed control loop instead of the measured rotor speed. The coordinate system transformation of the d-axis and q-axis is realized using the rotor flux angle estimated by the estimator. Sensorless drive operation at very low speeds and continuous variable speeds is considered to be a major problem for state-of-the-art estimators.

4.1. Sensorless speed tracking performance test

This test aims to verify the effective estimation ability of the speed sensorless RFOC based on the stator resistance deviation and the slip angular speed deviation mechanisms. The comparison of the operating curves of the estimated speed against the reference speed is shown in Fig. 7. The results show that the actual motor speed has good tracking performance for the reference speed in the range of 0-100rad/s. In Fig. 7(a), the effectiveness and robustness of the proposed speed sensor-less vector control can be seen from the motor speed operating curve. In Fig. 7(b), the comparison error between the estimated speed and the reference speed shows that the speed change is significant in a large range compared to a small range. In addition, from Fig. 7(b), it can be seen that the estimated speed can be tracked to the reference speed in a very short time by the estimation of the rotor speed estimator when the actual speed has a large error from the reference speed.

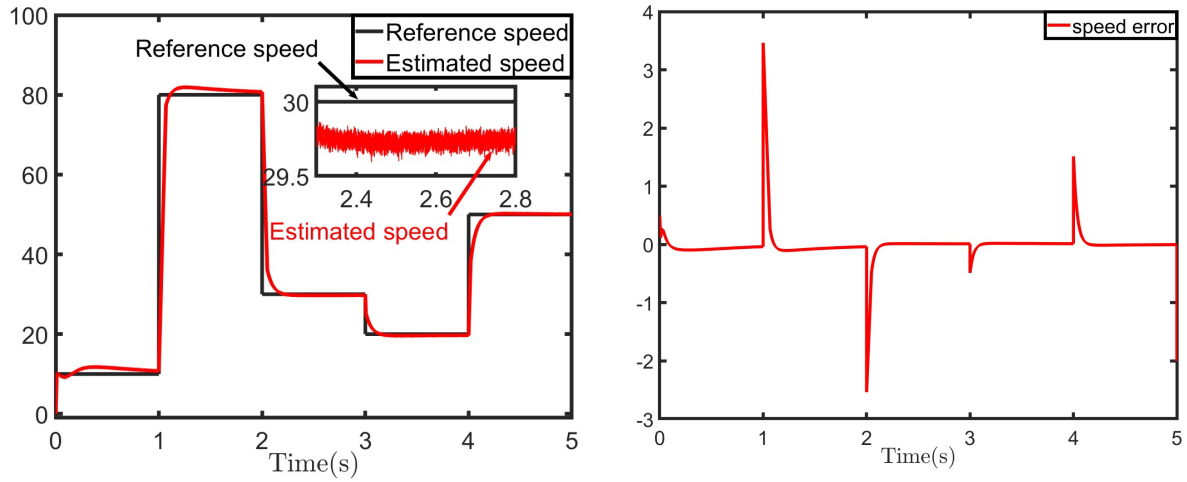

(a) (b)

Fig. 7: Sensorless speed tracking performance test. (a) Estimated speed and Reference speed (b) Speed error between reference speed and estimated speed

4.2. Sensitivity to the parameter variation test

In induction motor systems, the stator resistance is usually variable and uncertain because it varies with temperature and humidity during operation, especially in the motor windings [18],[27],[28]. In Fig. 8(a), the trajectory of the rotor speed is verified for different deviation of the stator resistance. The results show that the speed estimator performs the

same dynamic response when the stator resistance is deviate from its normal value by a constant mismatch value. Mismatch values with stator resistance deviations up to 50 are tested, and as can be seen from the plots, the speed estimation performance has been degraded with no significant change in the steady state. Obviously, it can also be found from Table 2a that the maximum value of speed error is 8.89 and the maximum mean absolute error is 6.9314. Both the curve in the figure and the data in the table indicate the effectiveness and feasibility of the stator voltage compensator. Therefore, in the case of stator resistance deviation, the stability and dynamic response performance of the speed estimator is still not affected as long as the stator voltage compensator is used.

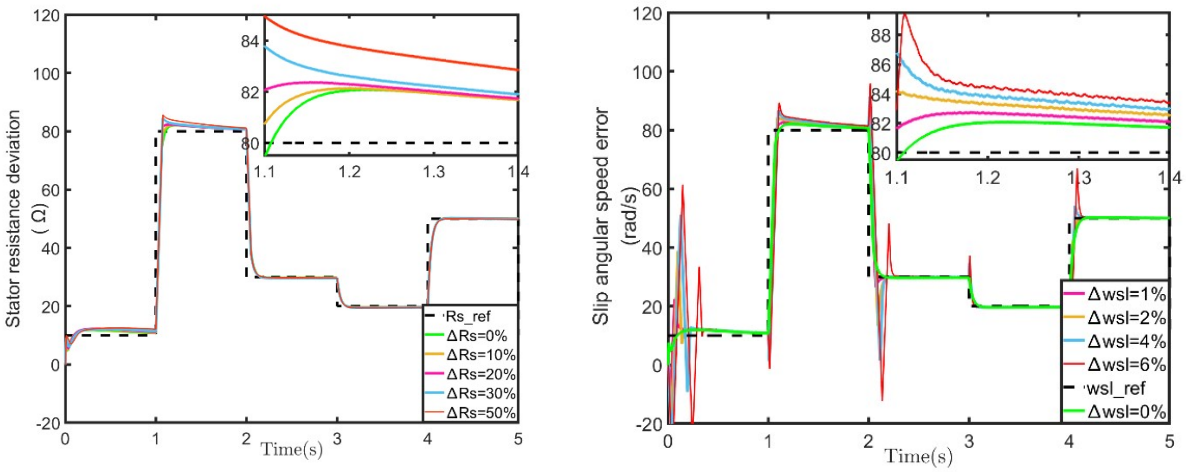

(a) (b)

Fig. 8: Simulink result of parameter variation sensitivity testing under (a) the stator resistance deviation (b) the slip angular speed deviation

Table 2a: Stator resistance deviation test

ΔR_s	Maximum error	Mean absolute error
10%	3.01	0.84889
20%	5.42	2.1519
30%	7.95	3.2294
50%	8.89	6.9314

Table 2b: Slip angular speed deviation test

$\Delta\omega_{sl}$	Maximum error	Mean absolute error
1%	38.12	10.9475
2%	41.34	16.3741
4%	49.07	38.9976
6%	51.93	43.2658

The slip angular speed is not obtained by direct measurement, but is estimated by PI controlling the error between the voltage model and current model of the rotor flux. Therefore, the estimation of the rotor speed is inevitably deviate. In Fig. 8(b), the trajectories

of rotor speed change are verified under different deviations of the slip angular speed. The results show that the rotor speed follows the reference speed well when the slip angular speed is deviated within a small range. However, the speed estimator is very sensitive to the deviation of the slip angular speed, which degrades the estimation performance in a slightly larger range. When the deviation of the test slip angular speed mismatch exceeds 6, the performance of the rotor speed estimator decreases dramatically and even destabilizes, which seriously affects the control performance of the system. From Table 2b, it will also be found that the maximum error of rotor speed reaches 51.93, and the maximum value of the average absolute error is 43.2658. Therefore, both the curve in the figure and the data in the table indicate that the slip angular speed mismatch can only occur in a very small range, or else it will affect the stability of the rotor speed estimator.

4.3. Speed tracking under zero load torque

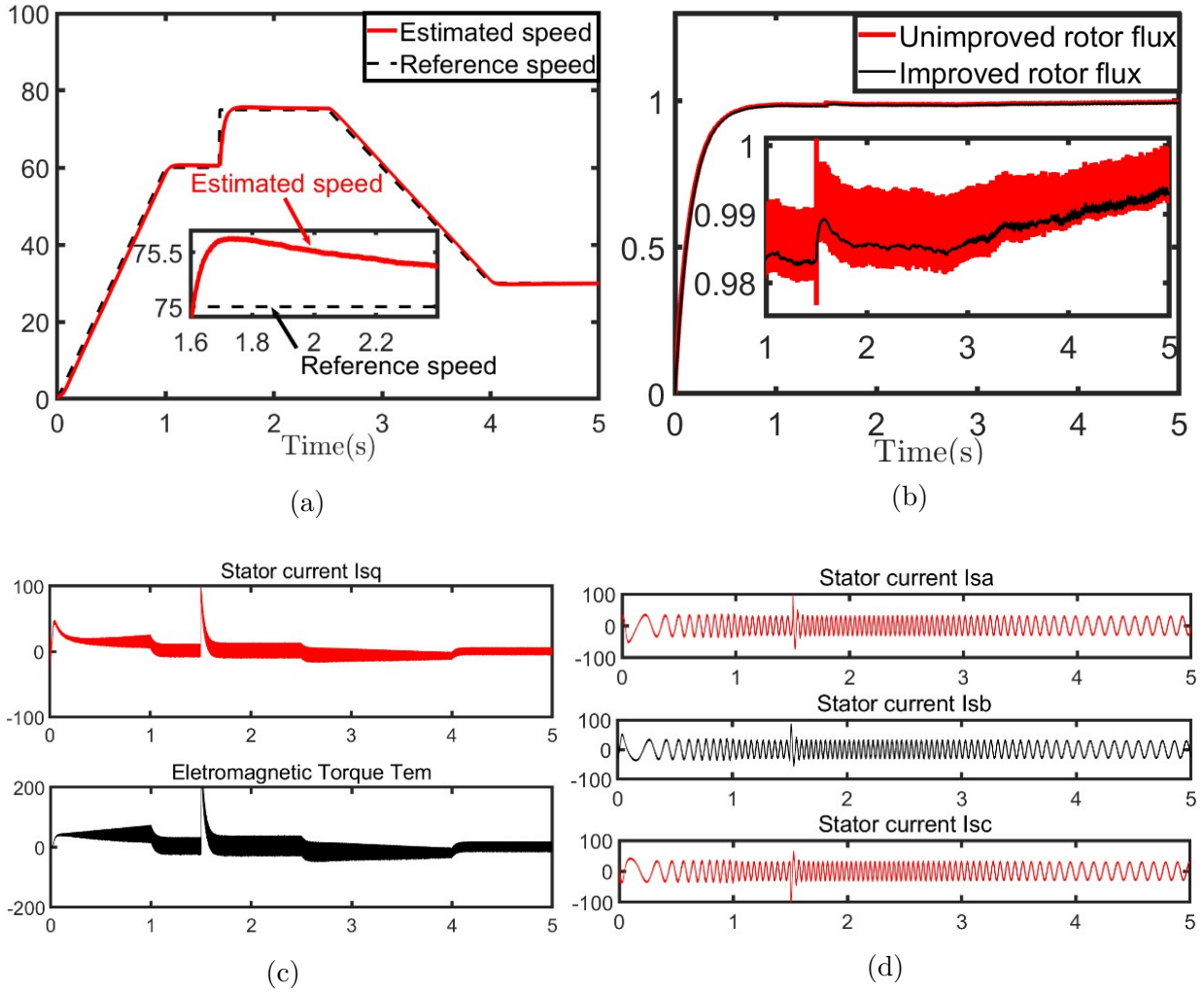

Fig. 9: Simulink results of IM speed tracking under zero load torque (a) Rotor speed (b) Improved and unimproved rotor flux (c) Stator current and Electromagnetic Torque (d) Stator current

Fig. 9(a) shows the results of the comparison between the estimated and reference speeds, and Fig. 9(b) shows the improved and unimproved d-axis estimated rotor flux, which responds to changes in speed. The d, q-axis components of the rotor flux are estimated from the induction motor rotor voltage model in the d, q coordinate system. The simulation results of the stator phase current measured by the sensor are given in Fig. 9(c). Fig. 9(d) shows the simulation results of the q-axis stator current and electromagnetic torque. All these simulation results are obtained for an induction motor system without speed sensors and load torque control, with a speed adjustment of 0-100r/min.

Some simulation results of sensorless speed control with speed control commands up to 100r/min are given in Fig. 9. In particular, very satisfactory performances of the induction motor have been achieved under the condition of applied load torque. The simulation results of motor speed, rotor flux, stator current and electromagnetic torque are given and the results are all in close agreement. Since the motor parameters are calculated based on the rated data, parameter shifts can lead to inaccurate calculation results. From Figures 9(a) and 9(b), it can be seen that the estimated rotor speed and rotor flux d-axis component errors occur for sudden changes in speed. It is clearly seen that the errors in the estimates of rotor speed and flux do not exceed 7% and 4%. The causes of this error have been analyzed and studied in the paper and are mainly due to parameter offsets and pure integration circuits. In order to avoid this situation, it is noticed from Fig. 9(b) that the estimation error of the rotor flux can be effectively reduced according to the stator voltage compensator algorithm.

It is worth to mention that the rotor resistance is considered constant. However, a similar phenomenon can also be found in the rotor resistance, which depends on the temperature and humidity at which the motor is operating. Only simulation studies have been carried out in the papers [27] and [28] to investigate the effect of the proposed method on the flux and torque decoupling and optimal control for variations in the rotor time constant parameter. It is clear that improvements in high-performance sensorless speed control also need to track changes in rotor resistance.

5. Conclusion

This manuscript investigates the issue of sensorless indirect rotor flux orientation control for induction motors with high dynamic performance in the presence of stator resistance deviation and slip angular velocity deviation. A stator voltage compensation method is proposed to suppress the voltage drop due to resistance deviation and to accurately estimate the flux as well as the flux angle. Subsequently, a speed estimator is designed to adjust the slip angular speed online in time to realize the method of online estimation of rotor flux and speed for induction motors. Simulation results show that the designed flux estimator has good dynamic performance and the estimated value is very close to the actual signal with an error of only 4%. In addition, the rotor speed estimator tracks the reference speed very accurately with an error of only 7%, which validates the effectiveness of the proposed method. The experimental results are contemplated as the future work. Some issues still exist, such as how to make the FOC design more robust and to accurately localize the flux angle in the presence of unknown parameter variations.

Acknowledgment

This work was supported by National Natural Science Foundation of China (U19A20110, 61863021) and Outstanding Talent Training Program of Lanzhou Jiaotong University (2022JC13).

[1] Imen Kortas, Anis Sakly, Mohamed Faouzi Mimouni. Optimal vector control to a double-star induction motor, Energy, 2018, 131:279-288.

[2] Yue Hanxue, Wang Huanqing, Wang Yueying. Adaptive fuzzy fixed-time tracking control for permanent-magnet synchronous motor, International Journal of Robust and Nonlinear Control, 2022, 32(5):3078-3095.

[3] Hicham Talhaoui, Arezki Menacer, Abdelhalim Kessal, Ridha Kechida. Fast fourier and discrete wavelet transforms applied to sensorless vector control induction motor for rotor bar faults diagnosis, ISA Transactions, 2014, 53(5):1639-1649.

[4] Tarek Ameid, Arezki Menacer, Hicham Talhaoui, Youness Azzoug. Discrete wavelet transform and energy eigen value for rotor bars fault detection in variable speed field-oriented control of induction motor drive, ISA Transactions, 2018, 79:217-231.

[5] Talib M, Ibrahim Z, Rahim N A. An improved simplified rules fuzzy logic speed controller method applied for induction motor drive, ISA Transactions, 2020, 105:230-239.

[6] Tobias Englert, Knut Graichen. Nonlinear model predictive torque control and setpoint computation of induction machines for high performance applications, Control Engineering Practice, 2020, 99:104415.

[7] Tianqing Wang, Bo Wang, Yong Yu. High-order sliding-mode observer with adaptive gain for sensorless induction motor drives in the wide-speed range, IEEE Transactions on Industrial Electronics, 2023, 70(11): 11055-11066.

[8] Mika Salo, Heikki Tuusa. A vector-controlled PWM current-source-inverter-fed induction motor drive with a new stator current control method, IEEE Transactions on Industrial Electronics, 2005, 52(2):523-531.

[9] Bo Wang, Tianqing Wang, Yong Yu. Second-order terminal sliding-mode speed controller for induction motor drives with nonlinear control gain, IEEE Transactions on Industrial Electronics, 2023, 70(11):10923-10934.

[10] Xie Fang, Qiu Chenming, Wang Qunjing, Liang Kangkang, Hong Weijie, Wu Wenming, Qian Zhe. The optimal speed-torque control of asynchronous motors for electric cars in the field-weakening region based on the RFR, IEEE Transactions on Industrial Electronics, 2020, 67(11):9601-9612.

[11] Cristian Lascu,Alin Argeseanu, Frede Blaabjerg. Super-twisting sliding mode direct torque and flux control of induction machine drives, IEEE Transactions on Power Electronics, 2020, 35(5):5057-5065.

[12] Shu Yamamoto, Hideaki Hirahara, Balapuwaduge Amith Sunasekara, Masayuki Motosugi. Stator-flux-linkage-calculation-based torque estimation of induction motors considering iron, mechanical, and stray load losses, IEEE Transactions on Industry Applications, 2021, 57(6):5916-5926.

[13] Angelo Accetta, Maurizio Cirrincione, Marrello Pucci, Antonino Sferiazza. State space-vector model of linear induction motors including end-effects and iron losses Part I: Theoretical Analysis, IEEE Transactions on Industry Applications, 2020, 56(1):235-244.

[14] Wang Huimin, Yang Yongheng, Chen Dunzhi, Ge Xinglai, Li Songtao, Zuo yun. Speed-sensorless control of induction motors with an open-loop synchronization method, IEEE Journal of Emerging and Selected Topics in Power Electronics, 2022, 10(2):1963-1977.

[15] Ding Jie, Chen Lijuan, Cao Zhengxin, Guo Honghao. Convergence analysis of the modified adaptive-extended Kalman filter for the parameter estimation of a brushless DC motor, International Journal of Robust and Nonlinear Control, 2021, 31:7606-7620.

[16] Jitendra Kr Jain, Sandip Ghosh, Somnath Maity, Pawel Dworak. PI controller design for indirect vector-controlled induction motor: A decoupling approach, ISA Transactions, 2017, 70:378-388.

[17] Jung Jinhwan, Nam Kwanghee. A dynamic decoupling control scheme for high-speed operation of induction motors, IEEE Transactions on Industrial Electronics, 1999, 46(1):100-110.

[18] Boussak Mohamed, Jarray Kamel. A high performance sensorless indirect stator flux orientation control of induction motor drive, IEEE Transactions on Industrial Electronics, 2006, 53(1):41-49.
[19] Zhang Shulin, Kang Jinsong, Yuan Jiawen. Analysis and suppression of oscillation in V/F controlled induction motor drive systems, IEEE Transactions on Transportation Electrification, 2022, 8(2):1566-1574.
[20] Abdelkarim Ammar, Aissa Kheldoun, Brahim Metidji. Feedback linearization based sensorless direct torque control using stator flux MRAS-sliding mode observer for induction motor drive, ISA Transactions, 2020, 98:382-392.
[21] Wang Huimin, Yang Yongheng, Ge Xinglai, Li Songtao, Zuo yun. Speed-sensorless control of linear induction motor based on the SSLKF-PLL speed estimation scheme, IEEE Transactions on Industry Applications, 2020, 56(5):4986-5002.
[22] Xue Yaru, Meng Dongyi, Yin Shaobo. Vector-based model predictive hysteresis current control for asynchronous motor, IEEE Transactions on Industrial Electronics, 2019, 66(11):8703-8712.
[23] Eftekhari Seyed Rasul, Davari Alireza, Naderi Peyman, Garcia Cristian, Rodriguez Jose. Robust loss minimization for predictive direct torque and flux control of an induction motor with electrical circuit model, IEEE Transactions on Power Electronics, 2020, 35(5):5417-5426.
[24] Zhang Yongchang, Yang Haitao. Model predictive torque control of induction motor drives with optimal duty cycle control, IEEE Transactions on Power Electronics, 2014, 29(12):6593-6603.
[25] Alkorta Patxi, Cortajarena José A, Barambones Oscar, Maseda Francisco. Effective generalized predictive control of induction motor, ISA Transactions, 2020, 103:295-305.
[26] Stender Marius, Wallscheid Oliver, Bŏecker Joachim. Accurate torque control for induction motors by utilizing a globally optimized flux observer, IEEE Transactions on Power Electronics, 2021, 36(11):13261-13274.
[27] Zaky Mohamed. A stable adaptive flux observer for a very low speed-sensorless induction motor drives insensitive to stator resistance variations, Ain Shams Engineering Journal, 2011, 2:11-20.
[28] Gou Lifeng, Wang Chenchen, Zhou Minglei, You Xiaojie. Integral sliding mode control for starting speed sensorless controlled induction motor in the rotating condition, IEEE Transactions on Power Electronics, 2020, 35(4):4105-4116.
[29] Ren Yaxing, Wang Ruotong, Rind Saqib Jamshed Rind, Zeng Pingliang, Lin Jiang. Speed sensorless nonlinear adaptive control of induction motor using combined speed and perturbation observer, Control Engineering Practice, 2022, 123:105166.
[30] Mapelli FL, Tarsitano D, Cheli F. MRAS rotor resistance estimators for EV vector-controlled induction motor traction drive: analysis and experimental results, Electric Power Systems Research, 2017, 146:298-307.
[31] Ameid Tarek, Menacer Arezki, Talhaoui Hicham, Harzelli Imadeddine. Rotor resistance estimation using extended Kalman filter and spectral analysis for rotor bar fault diagnosis of sensorless vector control induction motor, Measurement, 2017, 111:243-259.
[32] Nikpayam Mehdi, Ghanbari Mahmood, Esmaeli Abdolreza, Jannati Mohammad. Fault-tolerant control of Y-connected three-phase induction motor drives without speed measurement, Measurement, 2020, 149(7):106993.
[33] Zuo Yun, Ge Xinglai, Zheng Yuelei, Chen Yuexuan, Wang Huimin, Woldegiorgis Abebe Teklu, A Woldegiorgis. An adaptive active disturbance rejection control strategy for speed-sensorless induction motor drives, IEEE Transaction Transportation Electrification, 2022, 8(3):3336-3348.
[34] Gou Lifeng, Wang Chenchen, Zhou Minglei, You Xiaojie. Integral sliding mode control for starting speed sensorless controlled induction motor in the rotating condition, IEEE Transactions on power electronics, 2020, 35(4):4105-4116.
[35] Adrish Bhaumik, Sukanta Das. Virtual voltage vector based predictive current control of speed sensorless induction motor drives, ISA Transactions, 2023, 133:495-504.
[36] Wang Huimin, Yang Yongheng, Ge Xinglai, Zuo Yun, Chen Dunzhi. Speed-sensorless control of induction motor drives with a STA-FLL speed estimation scheme, IEEE Transaction on Industry Electronics, 2023, 70(12):12168-12180.

[37] Wang Huimin, Yang Yonghen, Ge Xinglai. PLL- and FLL-based speed estimation schemes for speed-sensorless control of induction motor drives: review and new attempts, IEEE Transactions on Power Electronics, 2022, 37(3):3334-3356.
[38] Golestan Saeed, Guerrero Josep, Vasquez Juan. Three-phase PLLs: a review of recent advances, IEEE Transactions on Power Electronics, 2017, 32(3):1894-1907.
[39] Yang Zebin, Ding Qifeng, Sun Xiaodong, Lu Chengling, Zhu Huimin. Speed sensorless control of a bearingless induction motor based on sliding mode observer and phase-locked loop, ISA Transactions, 2022, 123:346-356.
[40] Ortega R, Sarr A, Bobtsov A, Bahri I, Diallo D. Adaptive state observers for sensorless control of switched reluctance motors, International Journal of Robust and Nonlinear Control, 2019, 29(4):990-1006.
[41] Wang Mingyu, Chen Yangyu, Deng Wei, Wang Ruimiao. Rotor speed estimation for induction motor with stator and rotor resistances online identification, Electric Machines and Control, 2010, 14(4):66-71.
[42] Lascu Cristian, Andreescu Gheorghe Danniel. Sliding-mode observer and improved integrator with DC-offset compensation for flux estimation in sensorless-controlled induction motors, IEEE Transactions on Industrial Electronics, 2006, 53(3):785-794.